

Spin dynamics of triangular lattice antiferromagnet CuFeO_2 : Crossover from spin-liquid to paramagnetic phase

著者	Hayashi K., Nozaki T., Fukatsu R., Miyazaki Y., Kajitani T.
journal or publication title	Physical Review. B
volume	80
number	14
page range	144413
year	2009
URL	http://hdl.handle.net/10097/52968

doi: 10.1103/PhysRevB.80.144413

Spin dynamics of triangular lattice antiferromagnet CuFeO_2 : Crossover from spin-liquid to paramagnetic phase

K. Hayashi, T. Nozaki, R. Fukatsu, Y. Miyazaki, and T. Kajitani

Department of Applied Physics, Graduate School of Engineering, Tohoku University, Sendai 980-8579, Japan

(Received 20 May 2009; revised manuscript received 20 August 2009; published 19 October 2009)

We have investigated the spin dynamics of triangular lattice antiferromagnet CuFeO_2 by measuring powder neutron inelastic-scattering spectra. A quasielastic component whose half-width oscillates with the magnitude of the scattering vector appears in the spectra above Néel temperature. A dynamics model representing the shape of quasielastic components and oscillatory behaviors changes from spin jump diffusion to Heisenberg paramagnetic (PM) scattering with increasing temperature. These findings demonstrate that CuFeO_2 shows a gradual transition from a spin-liquid phase to the Heisenberg PM phase. The origin of the spin-liquid phase is discussed in terms of incommensurate short-range spin correlation.

DOI: [10.1103/PhysRevB.80.144413](https://doi.org/10.1103/PhysRevB.80.144413)

PACS number(s): 75.40.Gb

I. INTRODUCTION

Geometrically frustrated antiferromagnets of triangular, kagomé, and pyrochlore lattices have received considerable attention in recent years due to their extraordinary magnetic properties such as spin-liquid, spin-glass, and spin-ice phases.¹ Since the pioneering work by Anderson and Fazekas,² an antiferromagnetic (AF) Heisenberg model on the triangular lattice has been considered as a reasonable one for the spin-liquid phase in frustrated antiferromagnets. Although it is now believed that a magnetically ordered AF phase appears in the isotropic triangular lattice,^{3–7} recent theories^{1,8} suggest that exchange interactions beyond the nearest-neighbor sites such as the longer-range interactions, multiple-spin interactions, and incommensurate short-range correlation, may contribute to stabilize the spin-liquid phase in the triangular lattice. Experimentally, only a few candidates for spin-liquid phases have been reported in quantum spin systems ($S=1/2$) with a distorted triangular lattice^{9–11} and in a layered chalcogenide insulator NiGa_2S_4 with the exact triangular lattice of Ni spins ($S=1$).¹²

The delafossite-type oxide CuFeO_2 is a good example of the frustrated triangular lattice antiferromagnet due to its layered triangular lattices of high-spin Fe^{3+} ions. CuFeO_2 shows successive magnetic phase transitions from an Ising-type four-sublattice AF phase ($\uparrow\uparrow\downarrow\downarrow$) below Néel temperature $T_{N1} \sim 10.5$ K to a paramagnetic (PM) phase above $T_{N2} \sim 14.0$ K through a partially disordered (PD) phase ($T_{N1} < T < T_{N2}$).^{13–16} Despite the Heisenberg spin of the orbital singlet of Fe^{3+} magnetic ions ($L=0$, $S=5/2$), the thermal-induced magnetic transitions are well explained by the Ising model. The occurrence of the magnetic phase transitions is accompanied by second- and first-order structural phase transitions at T_{N2} and T_{N1} , respectively. CuFeO_2 changes from the hexagonal structure to a lower symmetry (monoclinic or orthorhombic) one below T_{N1} .^{17,18} Recently, some fascinating quantum phenomena such as field-induced multistep magnetization changes¹⁹ and multiferroics^{20–22} were found in this system. To understand these complicated magnetic properties, neutron inelastic-scattering measurements of CuFeO_2 and its diluted compounds were dedicated to reveal magnetic orderings and spin-wave excitations.^{23,24} However, a possible

spin-liquid phase of CuFeO_2 as a consequence of high ground-state spin degeneracy has received less attention.

Since the spin quantum number of Fe^{3+} ions in CuFeO_2 has a rather high value ($S=5/2$), the relevant phase should be primarily a classical spin-liquid phase. As proposed in an early work by Villain,²⁵ the pyrochlore Heisenberg antiferromagnet is a classical spin-liquid or cooperative paramagnet, i.e., an exchange-coupled paramagnet where spins have a diffusive motion. Theory predicted that at low T , being under the Weiss temperature Θ , the spin autocorrelation function would decay in time t as $\langle S_i(0) \cdot S_i(t) \rangle = \exp(-cTt)$, where c is a constant.²⁶ In this case, a quasielastic Lorentzian component appears in the neutron inelastic-scattering spectrum, which was confirmed experimentally in the pyrochlore CsNiCrF_6 .²⁷ This is also valid for the triangular lattice antiferromagnet because the lattice dimensionality seems to have very little effect on the dynamic magnetic response.²⁸ In fact, Simonet *et al.*²⁹ reported a quasielastic component in the powder neutron inelastic-scattering spectra of another delafossite-type oxide $\text{CuYO}_{2.5}$ at 150 and 300 K. By analyzing the spectrum at 300 K, they concluded that the origin of the quasielastic component was the Heisenberg PM scattering. Terada *et al.*²³ measured neutron inelastic-scattering spectra of single crystal CuFeO_2 at a specific scattering vector \mathbf{Q} in the PD phase and at 40 K, and presented a quasielastic component due to a diffusive magnetic excitation associated with strong spin fluctuations. More recently, Okuda *et al.*³⁰ found a low-energy magnetic excitation, i.e., a quasielastic component in the spectrum of delafossite-type oxide $\text{Cu}_{0.85}\text{Ag}_{0.15}\text{CrO}_2$ at $|\mathbf{Q}|=0.14 \text{ \AA}^{-1}$ just above T_N . Although they suggested a relation to many-body singlet excitations in a spin-liquid-like phase above T_N , no further identification was given concerning its origin.

In this work, we have succeeded in elucidating the spin dynamics of the spin-liquid phase by measuring the powder neutron inelastic-scattering spectra of CuFeO_2 at several temperatures. We find a quasielastic component above T_{N1} whose half-width Γ shows oscillation with $|\mathbf{Q}|$ for the first time. The quasielastic components below Θ are well fitted in terms of jump diffusion³¹ of Fe^{3+} spins, while those above Θ are attributed to the Heisenberg PM scattering.³² These results indicate a crossover from the PD phase to the spin-

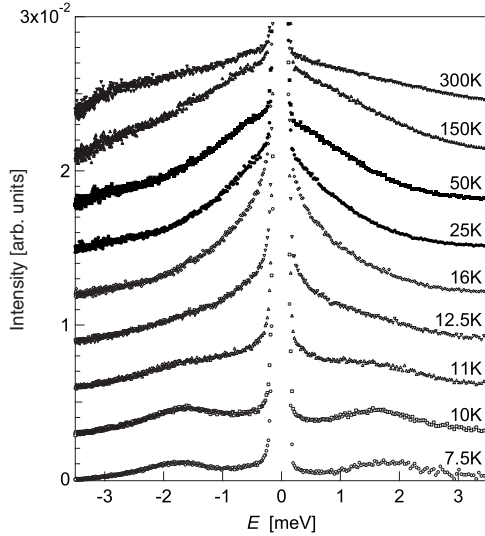


FIG. 1. Neutron inelastic-scattering spectra of CuFeO_2 powder with varying temperatures from 7.5 to 300 K.

liquid phase and finally to the PM phase with increasing temperature. In addition, we refer to a possibility that the spin autocorrelation function in the spin-liquid phase of geometrically frustrated antiferromagnets shows a $T^{1/2}$ dependency.

II. EXPERIMENT

Polycrystalline samples were prepared by a conventional solid-state reaction described elsewhere.³³ The x-ray diffraction pattern indicated that the sample had a delafossite structure without any impurity phases. The neutron inelastic-scattering measurements were carried out using a high-resolution pulsed neutron spectrometer AGNES, installed at the C3-1 cold neutron guide of JRR3M in Tokai, Japan.³⁴ A powder sample of about 10 g was loaded in a cylindrical aluminum cell (40 mm in height, 14.0 mm in inner diameter) sealed with an indium gasket. The incident neutrons with the wavelength of 4.22 Å were pulsed by a Fermi chopper, and scattered neutrons were detected by 328 detectors with a scattering angle of 10–130°, covering the scattering vector $|\mathbf{Q}|$ region of 0.20–2.70 Å⁻¹. The energy resolution was 0.12 meV at the energy-transfer values, E , of the incidence ranging from -4 to 4 meV. The data were collected at several temperatures in the range between 7.5 and 300 K. The duration of the measurements was about 24 h for each run. The neutron inelastic-scattering spectra presented below were symmetrized considering the differences in the up and down scatterings and geometrical conditions.

III. RESULTS AND DISCUSSION

Figure 1 shows neutron inelastic-scattering intensity, $S(E)$, representing the summation of $S(|\mathbf{Q}|, E)$ in the \mathbf{Q} space of CuFeO_2 . The horizontal axis is the energy-transfer values, E , of the incidence. The sharp central peaks at 0 meV are the elastic-scattering components. There is a large and broad inelastic peak around ± 2 meV in each spectrum below 11 K,

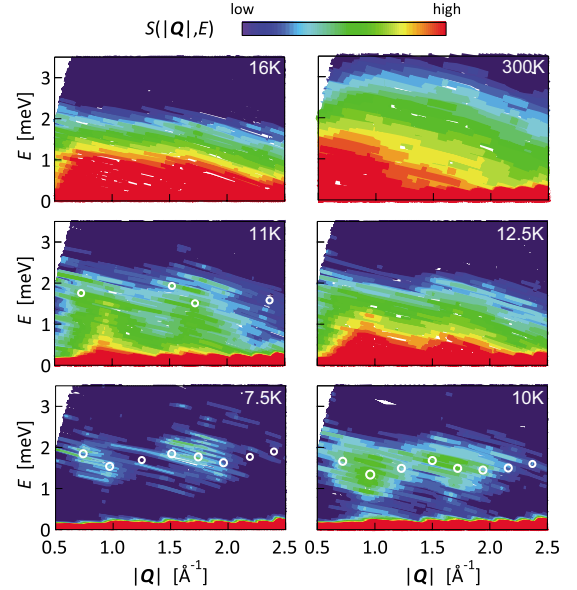


FIG. 2. (Color online) Intensity contour map of neutron inelastic scattering on CuFeO_2 powder at various temperatures. Circles are experimental data of the inelastic peak.

corresponding to the spin-wave excitations. As the temperature increases, the peak position moves closer to the central peak. The most important feature in this figure is a broad quasielastic component in each spectrum above 11 K. The maximum intensity of the quasielastic component is observed at 16 K just above T_{N2} , but the component decreases with increasing temperature. These results suggest that the spin dynamics changes from a wavelike regime to a diffusive one as the temperature increases.

We can see the change in more detail from the intensity contour map of $S(|\mathbf{Q}|, E)$ shown in Fig. 2. At 7.5 K, the low energy and almost dispersionless spin-wave branch is found at around 2 meV with an energy gap of ~ 1 meV, which is consistent with previous works.^{23,24} Reflecting the peak shift mentioned above, the energy of spin waves slightly decreases with increasing temperature. Above 11 K, it is difficult to find a clear spin-wave dispersion but instead, the quasielastic component appears in the whole $|\mathbf{Q}|$ range. Note that the half-width Γ of the quasielastic components seems to oscillate as a function of $|\mathbf{Q}|$, and the oscillatory behavior becomes less $|\mathbf{Q}|$ dependent with increasing temperature. A similar tendency is also observed in the intensity of the quasielastic components. The oscillation in the intensity becomes less evident above 150 K.

Hereafter we analyze the quasielastic component in the spectra above 12.5 K. As shown in Fig. 3(a), the quasielastic components below 50 K [region (I)] are well fitted to a Lorentzian function, taking the instrumental resolution function into account, whereas those at 150 and 300 K [region (II)] are fitted to a Gaussian function, also considering the resolution function. Thus the corresponding spin dynamics is different in region (I) and region (II). Figure 4 shows $|\mathbf{Q}|$ dependent Γ of the Lorentzian or Gaussian function. The oscillation amplitude and period are apparently different in region (I) and region (II). First, let us discuss the oscillatory behavior in region (I). This behavior cannot be explained by

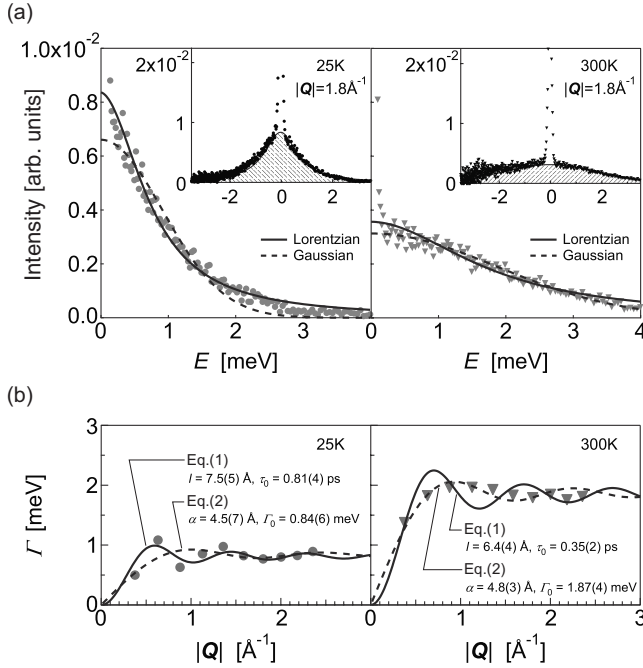


FIG. 3. Fitting results of (a) quasielastic components and (b) $|\mathbf{Q}|$ dependence of Γ of the quasielastic components at 25 and 300 K.

the theory for the pyrochlore Heisenberg antiferromagnet, which predicts that Γ is proportional to $|\mathbf{Q}|^2$.²⁶ An appropriate model that can explain the oscillation found in Γ of the Lorentzian function is the jump diffusion model, which is often used for the ionic impurity diffusion in liquids.³¹ Given

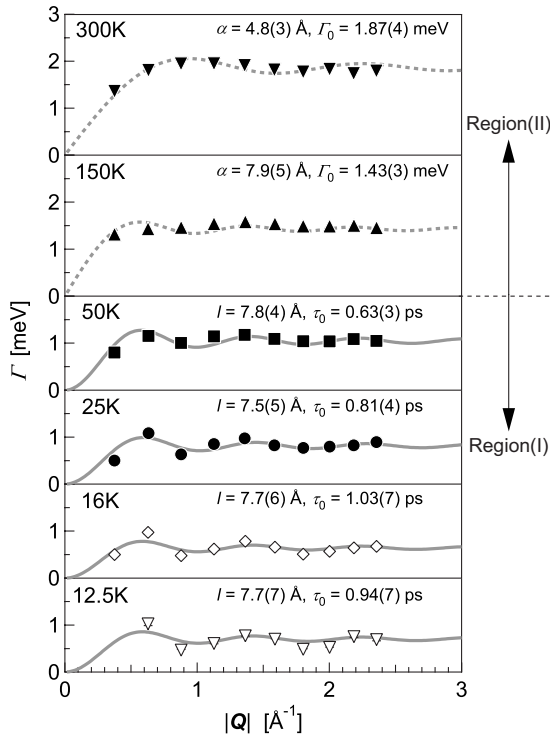


FIG. 4. $|\mathbf{Q}|$ dependence of Γ of the quasielastic components. The solid and dotted lines are fits to the models of jump diffusion and Heisenberg PM scattering, respectively.

that local spins jump at a fixed distance l from one pseudo-equilibrium Fe^{3+} site to another with the residence time τ between jumps, we obtain

$$\Gamma_L = \frac{\hbar}{\tau} \left(1 - \frac{\sin|\mathbf{Q}|l}{|\mathbf{Q}|l} \right). \quad (1)$$

The oscillatory behaviors are represented by Eq. (1) using a temperature dependent τ and a nearly constant $l \sim 7.7 \text{ \AA}$. The value of τ stays in the picosecond range, which is quite low relative to the precession frequency in CuCrO_2 , which stays at submicroseconds.³⁵ The jump distance l being longer than the triangular lattice spacing as well as the interlayer distance between the triangular lattices may correspond to the spin-correlation length.

In the PD phase, CuFeO_2 shows the incommensurate magnetic structure with sinusoidal amplitude modulation along the $\langle 110 \rangle$ direction with a period of $\sim 7.6 \text{ \AA}$,^{15,18} half of which is almost equal to l . Considering the two spins separated by a distance of $\sim 7.6 \text{ \AA}$, they are aligned ferromagnetically along the $\langle 110 \rangle$ direction and antiferromagnetically along the $\langle 100 \rangle$ or $\langle 010 \rangle$ direction. From this fact, we can expect that incommensurate AF short-range correlation due to such a magnetic ordering, which is characteristic for a triangular lattice Ising antiferromagnet, remains above T_{N2} . This expectation is also supported by magnetic-susceptibility measurements implying the development of short-range ordering below 150 K.¹⁴ Consequently, spins perform a diffusive jump to form antiparallel spin sites in the ab plane via AF exchange interactions. The growing intensity of the quasielastic component instead of the inelastic peaks with increasing temperature in the PD phase may indicate that the magnetic structure along the $\langle 110 \rangle$ direction in the PD phase is disturbed by the diffusive jump of spins. This spin dynamics due to the Ising-type short-range correlation may prevent possible formation of Z_2 vortices,³⁶ which has been recently proposed for the spin-liquid phase of the chalcogenide NiGa_2S_4 .³⁷ On the other hand, Petrenko *et al.*³⁸ claimed that the Ising model for CuFeO_2 was not applicable because the magnetic susceptibility measured in the field $H \parallel c$ and $H \perp c$ was almost isotropic above T_{N2} . In this case, the spin diffusion is not restricted to the ab plane. Although the detailed spin dynamics remains a matter of research, we tentatively conclude that the spin-liquid phase is realized in the region (I) probably due to the incommensurate short-range correlation. In other words, CuFeO_2 gradually changes from the PD phase to the spin-liquid phase around T_{N2} . This is strongly supported by other experimental facts such as a dull maximum in the magnetic susceptibility¹⁴ or a cusplike heat capacity³⁹ around T_{N2} .

Next we move on to discuss the $|\mathbf{Q}|$ dependence of Γ in region (II). The oscillatory behavior cannot be fitted to Eq. (1) as can be seen in the right side of Fig. 3(b). Since the temperature-dependent magnetic susceptibility of CuFeO_2 is described perfectly well by the Curie-Weiss law above 100 K (Ref. 38) or 150 K,¹⁴ the Heisenberg PM phase seems to be realized in region (II). Thus we attempt to explain the oscillatory behavior in terms of the Heisenberg PM scattering. According to the theory,³² the quasielastic component forms

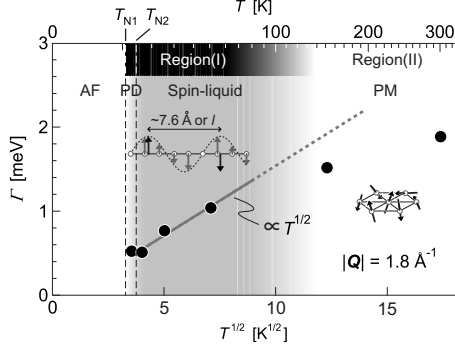


FIG. 5. Temperature dependence of Γ of the quasielastic components. Two schematics using the black arrows indicate possible spin structures for the spin-liquid (center) and PM (right) phases. In the schematic for the spin-liquid phase, the magnetic structure of the PD phase is also drawn with grey arrows.

a Gaussian function with the half-width Γ_G expressed as

$$\Gamma_G = \Gamma_0 \sqrt{1 - \frac{\sin|\mathbf{Q}|\alpha}{|\mathbf{Q}|\alpha}}, \quad \Gamma_0 \equiv \sqrt{\frac{2}{3}NS(S+1)} \cdot \frac{2J}{\hbar}, \quad (2)$$

where α , N , and J are the distance between nearest neighbors of Fe^{3+} ions, i.e., the in-plane lattice constant of 3.035 \AA ,³³ the number of nearest neighbors, and the exchange interaction, respectively. Here we treat α as well as Γ_0 as variable parameters to include long-range interactions. In the right side of Figs. 3(b) and 4, one can see that the oscillatory behavior in region (II) is reasonably explained by Eq. (2). On the other hand, the fitting of the oscillatory behavior in region (I) using Eq. (2) does not yield a good result as shown in the left side of Fig. 3(b). These results verify that CuFeO_2 is evidently in the Heisenberg PM phase in region (II). At 150 K, the value of α is as long as the jump distance l in region (I), and decreases by half at 300 K. The decrease in α corresponds to a gradual transition from the spin-liquid phase to the PM phase in CuFeO_2 . The transition may undergo at the Weiss temperature Θ of CuFeO_2 ($\sim 100 \text{ K}$).^{14,38,40} We believe that α becomes close to the distance between the nearest neighbors at higher temperature, i.e., the nearest-neighbor interactions become dominant.

Finally, we discuss the temperature-dependent change in Γ of CuFeO_2 . Since the temperature dependence of Γ is not strongly $|\mathbf{Q}|$ dependent, only the data at $|\mathbf{Q}| = 1.8 \text{ \AA}^{-1}$ are represented in Fig. 5. Although Γ at 11 K is not shown in the figure, it is larger than that at 12.5 K. The decreasing tendency of Γ in the PD phase as the temperature increases from T_{N1} to T_{N2} reflects the increase in τ , probably due to the development of local disorder induced by the increasing fraction of the spin-liquid phase in the PD phase. In the temperature range $T_{N2} < T < \Theta$, Γ increases with increasing temperature following a $T^{1/2}$ variation, not a T linear variation predicted in the pyrochlore Heisenberg antiferromagnet.²⁶ The deviation from a T linear variation was also found in the pyrochlore CsNiCrF_6 .²⁷ There is a possibility that the spin autocorrelation function for the spin-liquid phase of geometrically frustrated lattices is proportional to $T^{1/2}$. The $T^{1/2}$ variation is sometimes interpreted as a signature of the Kondo effect in heavy fermion systems;⁴¹ however, this is not the case for CuFeO_2 . Although Γ increases above Θ , its temperature variation deviates from that in the spin-liquid phase, an indication of the gradual transition from the spin-liquid phase to the PM phase. For deeper understanding of the spin dynamics of CuFeO_2 , triple-axis neutron inelastic-scattering experiments and further theoretical considerations are required. We note in passing that the Γ value of CuFeO_2 is comparable to those of the pyrochlore CsNiCrF_6 and other delafossite-type oxides $\text{CuYO}_{2.5}$ and $\text{Cu}_{0.85}\text{Ag}_{0.15}\text{CrO}_2$ (see, Table I). The Γ values are taken at certain temperatures between the magnetic transition temperatures T_0 and Θ except for $\text{CuYO}_{2.5}$.^{27,29,30} The magnetic phases and the types of spin dynamics are listed in Table I. Although $\text{CuYO}_{2.5}$ and $\text{Cu}_{0.85}\text{Ag}_{0.15}\text{CrO}_2$ are in the PM phase at low temperatures, there is a possibility that they are in the spin-liquid phase where spins perform the diffusive motion, which will be examined from the \mathbf{Q} dependence of quasielastic scattering intensities.

IV. CONCLUSION

We have measured neutron inelastic-scattering spectra of the delafossite-type oxide CuFeO_2 as a typical triangular lattice antiferromagnet. Due to the high-spin degeneracy of the

TABLE I. The half width Γ of the quasielastic component in the neutron inelastic-scattering spectrum of various frustrated materials at certain temperatures between the magnetic transition temperature T_0 and Θ except for $\text{CuYO}_{2.5}$.

	Γ	T_0	Θ	Magnetic phase	Spin dynamics
CuFeO_2 (This work)	0.8 meV ($ \mathbf{Q} = 1.8 \text{ \AA}^{-1}$, 25 K)	T_{N2}	$\sim 100 \text{ K}^a$	Spin-liquid	Jump diffusion
CsNiCrF_6^b	1 meV [$\mathbf{Q} = (2.5 \ 2.5 \ 0)$, 8.3 K]	2.3 K	100 \sim 300 K ^c	Spin-liquid	Diffusion
$\text{CuYO}_{2.5}^d$	1.5 meV ($ \mathbf{Q} = 1.8 \text{ \AA}^{-1}$, 150 K)	Unknown	$\sim 1 \text{ K}^e$	PM	
$\text{Cu}_{0.85}\text{Ag}_{0.15}\text{CrO}_2^f$	0.4 meV ($ \mathbf{Q} = 1.4 \text{ \AA}^{-1}$, 15 K)	13 K	160 K	PM	

^aRefs. 14, 38, and 40.

^bRef. 27.

^cRef. 42.

^dRef. 29.

^eRef. 43.

^fRef. 30.

ground state of CuFeO_2 , the spin-liquid phase is realized in the temperature range between T_{N1} and Θ . The spin-liquid phase is characterized in terms of the jump diffusion of spins, and the temperature dependence of the spin autocorrelation function obeys the $T^{1/2}$ variation. To our knowledge, CuFeO_2 is possibly the first spin-liquid material among the delafossite-type oxides. We expect that several delafossite-type oxides may also exhibit the spin-liquid behavior. Systematic study on their spin dynamics using the neutron inelastic-scattering measurements is underway.

ACKNOWLEDGMENTS

This work was partly supported by Grants-in-Aid for Scientific Research from the Ministry of Education, Culture, Sports, Science, and Technology of Japan, and also by ISSP, University of Tokyo (Grants No. 7657B and No. 8651B). We gratefully appreciate O. Yamamuro at ISSP, University of Tokyo for his help to measure the neutron inelastic-scattering spectra. One of us (K.H.) would like to thank M. Sasaki and H. Naganuma at Tohoku University for helpful discussions.

- ¹ *Frustrated Spin Systems*, edited by H. T. Diep (World Scientific, New York, 2004).
- ² P. W. Anderson, *Mater. Res. Bull.* **8**, 153 (1973); P. Fazekas and P. W. Anderson, *Philos. Mag.* **30**, 423 (1974).
- ³ B. Bernu, C. Lhuillier, and L. Pierre, *Phys. Rev. Lett.* **69**, 2590 (1992); B. Bernu, P. Lecheminant, C. Lhuillier, and L. Pierre, *Phys. Rev. B* **50**, 10048 (1994).
- ⁴ P. Sindzingre, P. Lecheminant, and C. Lhuillier, *Phys. Rev. B* **50**, 3108 (1994).
- ⁵ L. Capriotti, A. E. Trumper, and S. Sorella, *Phys. Rev. Lett.* **82**, 3899 (1999).
- ⁶ Z. Weihong, R. H. McKenzie, and R. R. P. Singh, *Phys. Rev. B* **59**, 14367 (1999).
- ⁷ S. Yunoki and S. Sorella, *Phys. Rev. B* **74**, 014408 (2006).
- ⁸ T. Kashima and M. Imada, *J. Phys. Soc. Jpn.* **70**, 3052 (2001).
- ⁹ Y. Shimizu, K. Miyagawa, K. Kanoda, M. Maesato, and G. Saito, *Phys. Rev. Lett.* **91**, 107001 (2003).
- ¹⁰ T. Itou, A. Oyamada, S. Maegawa, M. Tamura, and R. Kato, *Phys. Rev. B* **77**, 104413 (2008).
- ¹¹ R. Coldea, D. A. Tennant, A. M. Tsvelik, and Z. Tylczynski, *Phys. Rev. Lett.* **86**, 1335 (2001).
- ¹² S. Nakatsuji, Y. Nambu, H. Tonomura, O. Sakai, S. Jonas, C. Broholm, H. Tsunetsugu, Y. Qiu, and Y. Maeno, *Science* **309**, 1697 (2005).
- ¹³ S. Mitsuda, H. Yoshizawa, N. Yaguchi, and M. Mekata, *J. Phys. Soc. Jpn.* **60**, 1885 (1991).
- ¹⁴ M. Mekata, N. Yaguchi, T. Takagi, T. Sugino, S. Mitsuda, H. Yoshizawa, N. Hosoito, and T. Shinjo, *J. Phys. Soc. Jpn.* **62**, 4474 (1993).
- ¹⁵ S. Mitsuda, N. Kasahara, T. Uno, and M. Mase, *J. Phys. Soc. Jpn.* **67**, 4026 (1998).
- ¹⁶ N. Terada, T. Kawasaki, S. Mitsuda, H. Kimura, and Y. Noda, *J. Phys. Soc. Jpn.* **74**, 1561 (2005).
- ¹⁷ N. Terada, S. Mitsuda, H. Ohsumi, and K. Tajima, *J. Phys. Soc. Jpn.* **75**, 023602 (2006).
- ¹⁸ F. Ye, Y. Ren, Q. Huang, J. A. Fernandez-Baca, P.-C. Dai, J. W. Lynn, and T. Kimura, *Phys. Rev. B* **73**, 220404(R) (2006).
- ¹⁹ Y. Ajiro, T. Asano, T. Takagi, M. Mekata, H. Aruga-Katori, and T. Goto, *Physica B* **201**, 71 (1994); Y. Ajiro, K. Hanasaki, T. Asano, T. Takagi, M. Mekata, H. Aruga-Katori, and T. Goto, *J. Phys. Soc. Jpn.* **64**, 3643 (1995).
- ²⁰ T. Kimura, J. C. Lashley, and A. P. Ramirez, *Phys. Rev. B* **73**, 220401(R) (2006).
- ²¹ S. Kanetsuki, S. Mitsuda, T. Nakajima, D. Anazawa, H. A. Katori, and K. Prokes, *J. Phys.: Condens. Matter* **19**, 145244 (2007).
- ²² S. Seki, Y. Yamasaki, Y. Shiomi, S. Iguchi, Y. Onose, and Y. Tokura, *Phys. Rev. B* **75**, 100403 (2007)(R)
- ²³ N. Terada, S. Mitsuda, Y. Oohara, H. Yoshizawa, and H. Takei, *J. Magn. Magn. Mater.* **272-276**, e997 (2004); N. Terada, S. Mitsuda, T. Fujii, and D. Petitgrand, *J. Phys.: Condens. Matter* **19**, 145241 (2007).
- ²⁴ F. Ye, J. A. Fernandez-Baca, R. S. Fishman, Y. Ren, H. J. Kang, Y. Qiu, and T. Kimura, *Phys. Rev. Lett.* **99**, 157201 (2007).
- ²⁵ J. Villain, *Z. Phys. B* **33**, 31 (1979).
- ²⁶ R. Moessner and J. T. Chalker, *Phys. Rev. Lett.* **80**, 2929 (1998).
- ²⁷ M. J. Harris, M. P. Zinkin, and T. Zeiske, *Phys. Rev. B* **52**, R707 (1995).
- ²⁸ B. Canals and D. A. Garanin, *Can. J. Phys.* **79**, 1323 (2001).
- ²⁹ V. Simonet, R. Ballou, A. P. Murani, O. Garlea, C. Darie, and P. Bordet, *J. Phys.: Condens. Matter* **16**, S805 (2004).
- ³⁰ T. Okuda, T. Kishimoto, K. Uto, T. Hokazono, Y. Onose, Y. Tokura, R. Kajimoto, and M. Matsuda, *J. Phys. Soc. Jpn.* **78**, 013604 (2009).
- ³¹ C. T. Chudley and R. J. Elliott, *Proc. Phys. Soc. London* **77**, 353 (1961).
- ³² P. G. de Gennes, *J. Phys. Chem. Solids* **4**, 223 (1958).
- ³³ K. Hayashi, T. Nozaki, and T. Kajitani, *Jpn. J. Appl. Phys.* **46**, 5226 (2007).
- ³⁴ T. Kajitani, K. Shibata, S. Ikeda, M. Kohgi, H. Yoshizawa, K. Nemoto, and K. Suzuki, *Physica B* **213-214**, 872 (1995).
- ³⁵ Y. Ikedo, J. Sugiyama, H. Nozaki, K. Mukai, P. L. Russo, D. Andreica, A. Amato, Y. Ono, and T. Kajitani, *Physica B* **404**, 645 (2009).
- ³⁶ H. Kawamura and S. Miyashita, *J. Phys. Soc. Jpn.* **53**, 4138 (1984); H. Kawamura, *J. Phys.: Condens. Matter* **10**, 4707 (1998).
- ³⁷ H. Kawamura and A. Yamamoto, *J. Phys. Soc. Jpn.* **76**, 073704 (2007).
- ³⁸ O. A. Petrenko, M. R. Lees, G. Balakrishnan, S. de Brion, and G. Chouteau, *J. Phys.: Condens. Matter* **17**, 2741 (2005).
- ³⁹ K. Takeda, K. Miyake, M. Hitaka, T. Kawae, N. Yaguchi, and M. Mekata, *J. Phys. Soc. Jpn.* **63**, 2017 (1994).
- ⁴⁰ J.-P. Doumerc, A. Wichainchai, A. Ammar, M. Pouchard, and P. Hagenmuller, *Mater. Res. Bull.* **21**, 745 (1986).
- ⁴¹ N. E. Bickers, D. L. Cox, and J. W. Wilkins, *Phys. Rev. B* **36**, 2036 (1987).
- ⁴² E. Banks, J. A. Deluca, and O. Berkooz, *J. Solid State Chem.* **6**, 569 (1973).
- ⁴³ K. Isawa, Y. Yaegashi, M. Komatsu, M. Nagano, S. Sudo, M. Karppinen, and H. Yamauchi, *Phys. Rev. B* **56**, 3457 (1997).